Stochastic ERK Activation Induced by Noise and Cell-to-Cell Propagation Regulates Cell Density-Dependent Proliferation

Kazuhiro Aoki,[1,*] Yuka Kumagai,[2] Atsuro Sakurai,[2] Naoki Komatsu,[2] Yoshihisa Fujita,[3] Clara Shionyu,[2] and Michiyuki Matsuda[2,3]
[1]Imaging Platform for Spatio-Temporal Information, Graduate School of Medicine, Kyoto University, Sakyo-ku, Kyoto 606-8501, Japan
[2]Laboratory of Bioimaging and Cell Signaling, Graduate School of Biostudies, Kyoto University, Sakyo-ku, Kyoto 606-8501, Japan
[3]Department of Pathology and Biology of Diseases, Graduate School of Medicine, Kyoto University, Sakyo-ku, Kyoto 606-8501, Japan
*Correspondence: k-aoki@lif.kyoto-u.ac.jp
http://dx.doi.org/10.1016/j.molcel.2013.09.015

SUMMARY

The extracellular signal-regulated kinase (ERK) plays a central role in the signaling cascades of cell growth. Here, we show that stochastic ERK activity pulses regulate cell proliferation rates in a cell density-dependent manner. A fluorescence resonance energy transfer (FRET) biosensor revealed that stochastic ERK activity pulses fired spontaneously or propagated from adjacent cells. Frequency, but not amplitude, of ERK activity pulses exhibited a bell-shaped response to the cell density and correlated with cell proliferation rates. Consistently, synthetic ERK activity pulses generated by a light-switchable CRaf protein accelerated cell proliferation. A mathematical model clarified that 80% and 20% of ERK activity pulses are generated by the noise and cell-to-cell propagation, respectively. Finally, RNA sequencing analysis of cells subjected to the synthetic ERK activity pulses suggested the involvement of serum responsive factor (SRF) transcription factors in the gene expression driven by the ERK activity pulses.

INTRODUCTION

Cell proliferation is a highly regulated process that maintains tissue architectures and organ size in multicellular organisms (Eagle and Levine, 1967). The inhibition of cell proliferation observed in confluent cells is referred to as contact inhibition of proliferation, or simply contact inhibition, and a defect of this process has been closely associated with uncontrolled cell proliferation during tumorigenesis (Abercrombie, 1979). Although accumulating evidence suggests that E-cadherin-mediated cell-cell contact induces contact inhibition (Navarro et al., 1991; St Croix et al., 1998), the intracellular signaling machinery that embodies growth inhibition seems to be multifaceted and dependent on cellular context. For example, downregulation of extracellular signal-regulated kinase (ERK) mitogen-activated protein kinase (MAPK) is manifested in confluent monolayers of fibroblasts (Wayne et al., 2006), epithelial cells (Li et al., 2004),

and vascular endothelial cells (Viñals and Pouysségur, 1999). Furthermore, it has been reported that E-cadherin stimulates cell proliferation via the Rac1 small guanosine triphosphatase (GTPase) at an intermediate cell density (Liu et al., 2006).

The ERK MAPK is a serine/threonine kinase that serves as the output of the Ras-Raf-MEK-ERK signal transduction pathway (Nishida and Gotoh, 1993). Upon Ras activation, which could be triggered by a number of growth factors or differentiation factors, Raf is recruited to Ras at the plasma membrane. The Ras-Raf complex activates MEK, which in turn phosphorylates tyrosine and threonine residues in the activation loop of ERK in the cytoplasm. The activated ERK catalyzes the phosphorylation of many downstream proteins, thereby regulating a large variety of cellular processes, including cell proliferation, differentiation, and tumorigenesis (Qi and Elion, 2005; Roskoski, 2012).

Differences in the kinetics of signaling molecules, including protein kinases, have been suggested to dictate appropriate outcomes in diverse biological systems (Marshall, 1995). For example, sustained ERK activation for at least several hours is required for the induction of genes, such as cyclin D, and consequent entry into S phase (Kahan et al., 1992; Pagès et al., 1993). This phenomenon could be explained by the observation that sustained ERK activity is required for stabilization of the c-Fos protein and cell cycle entry (Murphy et al., 2002). On the other hand, in PC12 pheochromocytoma cells, sustained ERK activation inhibits cell growth and induces neuronal differentiation (Sasagawa et al., 2005). These are good examples that the duration of signaling molecules' activation modulates the cellular function. Recently, owing to the advent of fluorescent proteins and their application, which has enabled us to observe the single-cell dynamics of signaling molecules, the frequency of transcription factors' activation has been shown to modulate gene expression (Cai et al., 2008; Hao and O'Shea, 2012). More recently, epidermal growth factor (EGF) has been shown to induce ERK activation pulses, the frequency of which depends on the concentration of EGF and controls the velocity of cell proliferation in mammary epithelial cells (Albeck et al., 2013). However, it has not been directly demonstrated how such dynamic behavior of ERK activity is processed and decoded to alter cellular function at different cell densities.

Here, we demonstrate that the frequency of stochastic ERK activity pulses controls the proliferation rate in a cell density-dependent manner. The stochastic dynamics of ERK activation
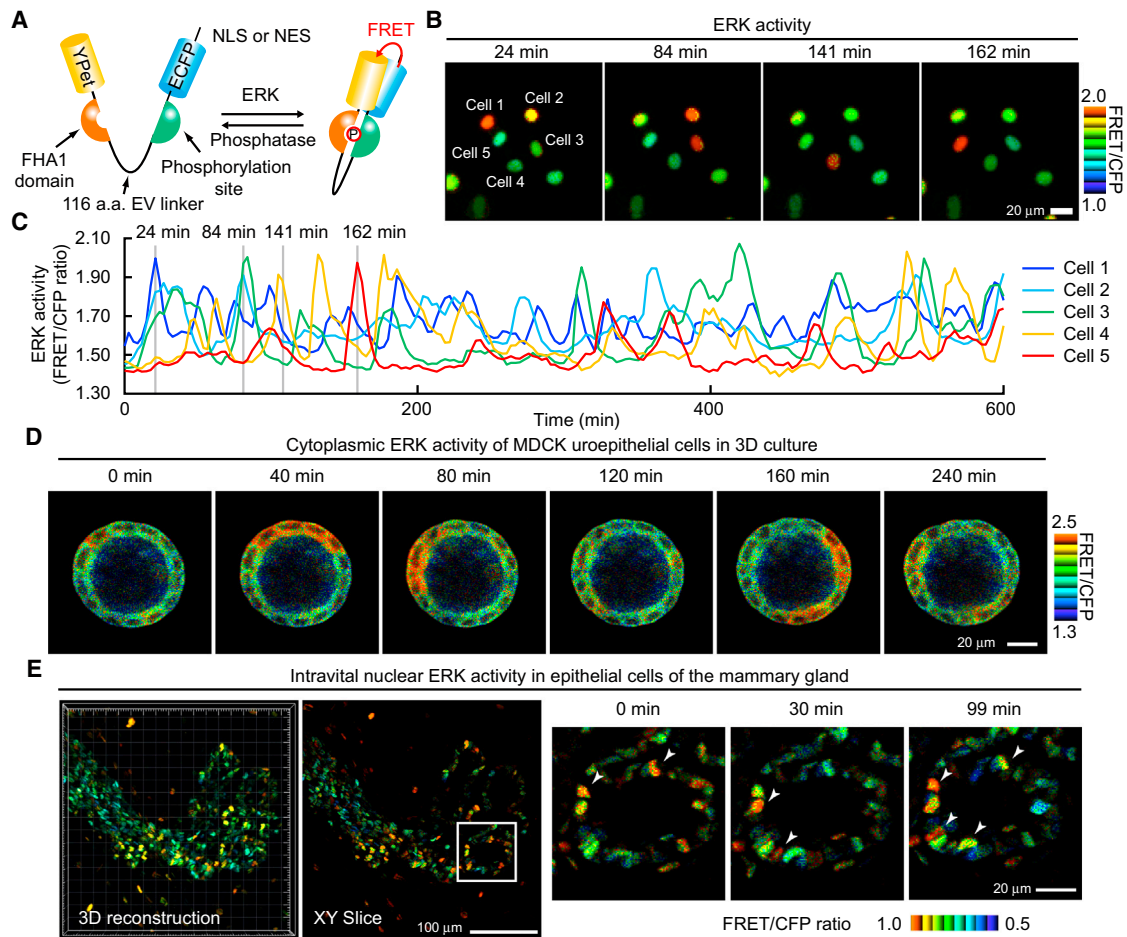
Figure 1. Correlation of the Cell Density-Dependent Stochastic ERK Dynamics and Cell Proliferation

(A) Schematic of the structure of the FRET biosensor for ERK activity, EKAREV-NLS. NLS is the nuclear localization sequence.

(B and C) NRK-52E cells stably expressing EKAREV-NLS were cultured in the presence of 10% FBS and imaged with epifluorescence microscopy (B). FRET/CFP ratio images at the indicated time points are shown in intensity-modulated display (IMD) mode. FRET/CFP ratios in the indicated cells are plotted as a function of elapsed time (C). Gray lines correspond to the time point in (B).

(D) ERK activity in XY slices of cysts in MDCK cells expressing EKAREV-NES are represented in the IMD mode.

(E) The mammary glands in 12-week-old female mice expressing EKAREV-NLS were observed by two-photon excitation microscopy. A reconstituted 3D structure of the mammary glands (left), the XY slice (center), and enlarged images (right) are shown in the IMD mode. Arrow heads represent the nuclei of cells showing stochastic ERK activation. See also Figure S1.

were visualized by an ERK biosensor, EKAREV, based on the principle of fluorescence resonance energy transfer (FRET) (Komatsu et al., 2011), revealing that the ERK activity pulses were fired spontaneously or propagated from adjacent cells. We found a biphasic pattern in the relationship between the frequency of ERK activity pulses and cell density. Synthetic ERK oscillation using a light-switchable ERK activation system increased the cell proliferation. Finally, RNA sequencing (RNA-seq) analysis revealed several genes that were specifically induced by the ERK activity pulses.

RESULTS

FRET Imaging Reveals Stochastic ERK Activity Pulses

We recently reported a highly sensitive ERK FRET biosensor, EKAREV, and a protocol to establish cell lines stably expressing FRET biosensors (Aoki et al., 2012). EKAREV was shown to monitor ERK activity as low as 5% (Figure S1A, available online). This success led us to examine the basal ERK activity in individual cells over a long period (Figures 1A and 1B, Movie S1). Time-lapse FRET imaging of normal rat kidney epithelial (NRK-52E) cells revealed that each cell exhibited stochastic ERK activity pulses in the presence of 10% fetal bovine serum (FBS) in culture medium (Figure 1C). The peak amplitude of ERK activation pulse corresponded to ERK activation induced by 1–2 nM 12-O-Tetra-decanoylphorbol 13-acetate (TPA) (Figures S1B and S1C). Similar stochastic ERK activity pulses could be detected in a wide range of cells, including HeLa cells, Cos7 cells, and mouse embryonic fibroblasts, but not in other cells, including Colo205 cells and Jurkat T cells (Figure S1D). A cyst of Madin-Darby canine kidney (MDCK) cells cultured in three-dimensional (3D) cell culture in a gel, which reconstituted the in vivo
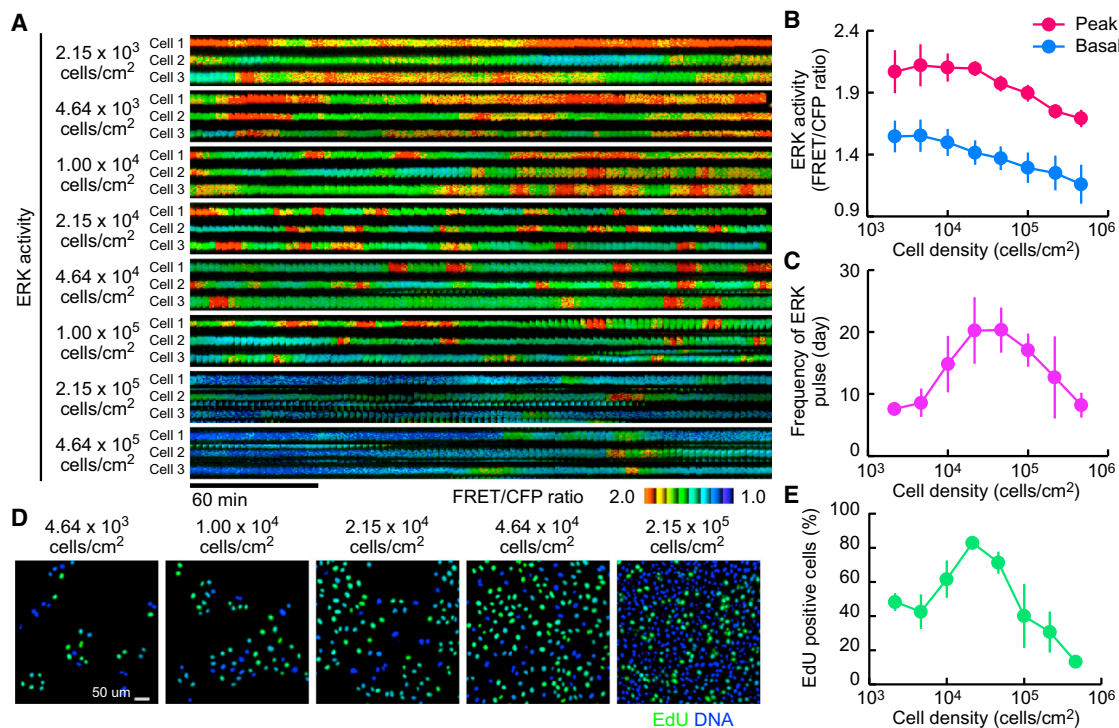
Figure 2. Correlation of the Cell Density-Dependent Stochastic ERK Dynamics and Cell Proliferation

(A) NRK-52E cells expressing EKAREV-NLS were imaged as in Figures 1B and 1C. Montage images of the nucleus in three representative cells are shown in the IMD mode.

(B and C) Averaged basal and peak ERK activity pulses (B) and frequency of ERK activity pulses (C) were quantified and plotted as a function of cell density with SD (n = 3).

(D and E) Cell density-dependent proliferation rate in NRK-52E cells were analyzed for EdU incorporation. Percentage of EdU-positive cells are represented as mean with SD. See also Figure S2.

microenvironment, also demonstrated stochastic ERK activity pulses (Figure 1D, Movie S2). Furthermore, intravital two-photon imaging revealed that ERK was stochastically and transiently activated in epithelial cells of mammary glands (Figure 1E, Movie S3), suggesting general roles of stochastic ERK activity pulses in vivo. Meanwhile, we noticed that the FRET/CFP value increased around the M phase even in the presence of an MEK inhibitor (Figures S1E and S1F). The cyclin B/CDK1 complex may phosphorylate EKAREV in the M phase because the ERK substrate sequence in EKAREV shares a consensus phosphorylation sequence of CDK1 substrates. Therefore, we omitted the data of the M phase from the following analysis and confirmed the observation of the interphase by specific MEK inhibitors.

Cell Density Affects the Frequency of ERK Activity Pulses

During the course of the experiments, we noticed a significant correlation between cell density and the frequency of ERK activity pulses. Therefore, we further investigated the effect of cell density on the frequency of ERK activity pulses in NRK-52E cells. Cells were plated on glass base dishes from a density at which cells were mostly isolated (2.2×10^3 cells/cm^2) to a density at which cells were confluent (4.6×10^5 cells/cm^2). On the next day, cells were time-lapse imaged for 4 hr (Figure 2A, Movie S4). Kymographic FRET images revealed that basal ERK activity

decreased with increasing cell density (Figure 2B) and the frequency of the ERK activity pulses exhibited a bell-shaped response to cell density, with a highest peak at intermediate cell density ($2.2–4.6 \times 10^4$ cells/cm^2) (Figure 2C). Notably, the averaged width of each activity pulse, approximately 20 min, was not significantly affected by the cell density. We also noticed that the ERK activity pulses were often propagated to the neighboring cells at the intermediate cell density.

To examine the correlation between ERK activity and the cell proliferation rate, NRK-52E cells were analyzed by an 5-ethynyl-20-deoxyuridine (EdU) incorporation assay (Figure 2D). In agreement with a previous work (Liu et al., 2006), we found that NRK-52E cells at sparse densities ($2.2–4.6 \times 10^3$ cells/cm^2) replicated more slowly than those at an intermediate cell density, at which most cells were in contact with one or two neighboring cells (2.2×10^4 cells/cm^2). On the other hand, cells approaching confluence underwent contact inhibition of growth ($\sim 2.2 \times 10^5$ cells/cm^2) (Figure 2E). By comparing Figures 2B, 2C, and 2F, we noted that the frequency of ERK activity pulses, but not the basal ERK activity, was strongly correlated with the replication rate of cells. In line with these results, increasing serum concentration in culture medium augmented not only basal ERK activity (Figure S2A), but also the frequency of ERK activity pulses (Figure S2B), accompanied by the increment of cell proliferation rate (Figure S2C).
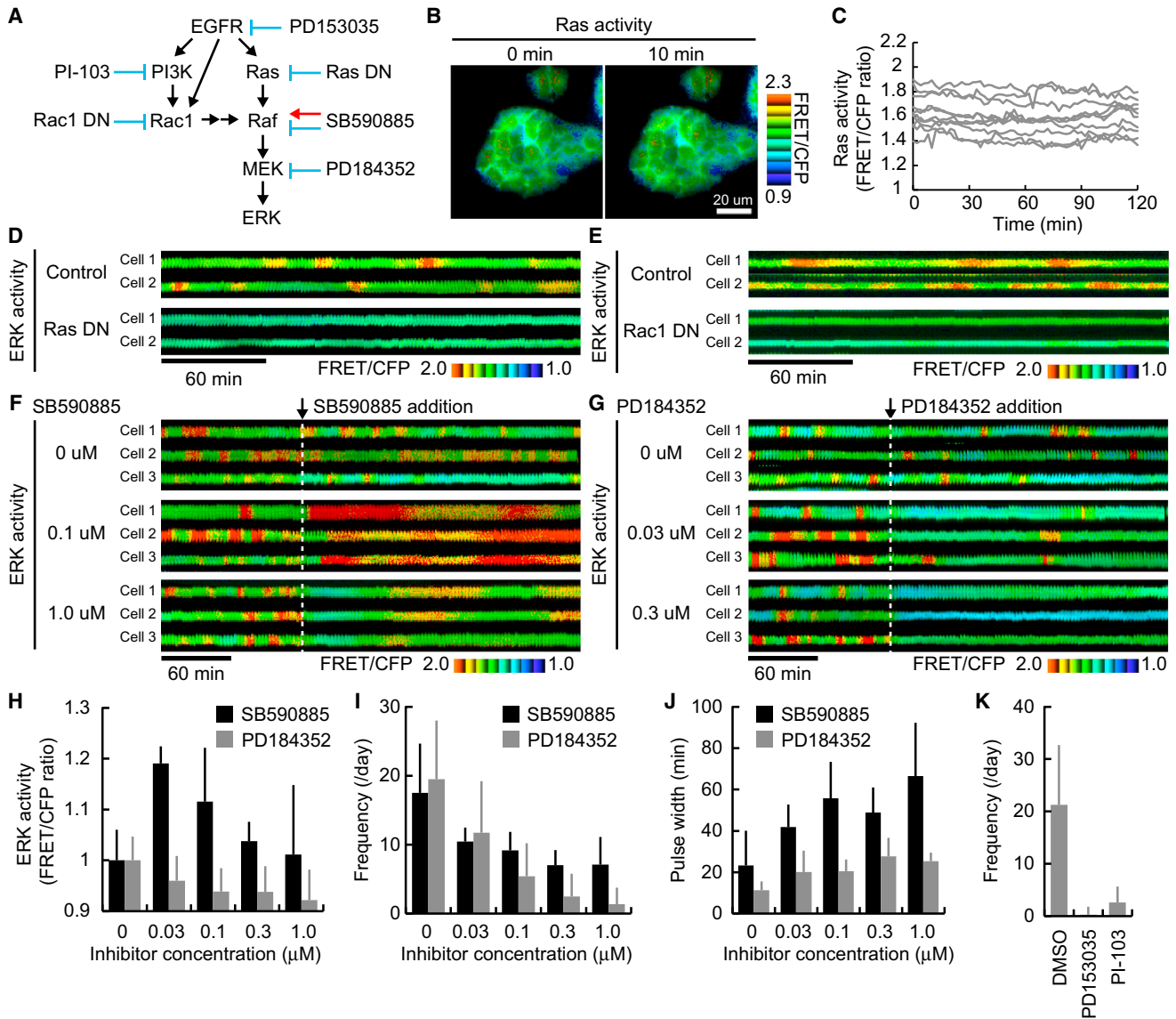
Figure 3. Perturbation Analysis Suggested a Role for Raf as a Pulse Generator

(A) A schematic of the EGFR-Ras-ERK cascade with inhibitors.

(B and C) Ras activity was visualized by RaichuEV-Ras in NRK-52E cells cultured with 10% FBS (B), showing no detachable stochastic change (C).

(D) Montage images of ERK activity in the control (upper) or dominant-negative mutant of Ras (Ras DN)-expressing (lower) NRK-52E cells stably expressing EKAREV-NLS (NRK-52E cells/EKAREV-NLS).

(E) Montage images of ERK activity in the control (upper) or dominant-negative mutant of Rac1 (Rac1 DN)-expressing (lower) NRK-52E cells/EKAREV-NLS.

(F and G) Montage images of ERK activity are shown in NRK-52E cells expressing EKAREV-NLS treated with DMSO, SB590885 (F), and PD184352 (G) under the condition of 10% FBS.

(H–J) Basal ERK activity (H), frequency of ERK activity pulses (I), and pulse width (J) are shown as mean with SD (n = 17, 26, 44, 47, and 36 for SB590558; n = 93, 93, 95, 104, and 114 for PD184352).

(K) Frequency of ERK activity pulses in the presence of DMSO (n = 51), 1 μM PD153035 (EGFR inhibitor, n = 78), and 10 μM PI-103 (PI3K inhibitor, n = 63) are shown as mean with SD. See also Figure S3.

Raf Is Involved in the Generation of Stochastic ERK Activity Pulse

The aforementioned results prompted us to investigate the molecular mechanisms underlying the stochastic ERK activity pulses by dominant-negative mutants or chemical inhibitors in the Ras-ERK pathway (Figure 3A). First, FRET imaging with RaichuEV-Ras, a FRET biosensor for Ras (Komatsu et al., 2011), demonstrated that Ras did not show stochastic activity pulses as did ERK (Figures 3B and 3C). Nevertheless, a dominant-negative mutant of Ras, Ras DN, completely blocked the stochastic ERK activity

pulses (Figure 3D). RaichuEV-Ras was sensitive enough to monitor the basal Ras activity, as evidenced by a reduced FRET/CFP ratio in Ras DN-expressing cells (Figures S3A and S3B). These results strongly suggest that the basal Ras activity is a prerequisite for the stochastic ERK activity pulses but that Ras itself did not generate pulsatile activation. Rac1, a member of Rho family GTPases, has been reported to be involved in E-cadherin-mediated cell proliferation (Liu et al., 2006). In agreement with this report, a Rac1 dominant-negative mutant, Rac1 DN, also substantially suppressed the stochastic ERK activity pulses (Figure 3E).

Second, we examined the effect of chemical inhibitors of Raf and MEK (Figures 3F–3J). ERK activity demonstrated a biphasic dose response to a potent Raf inhibitor, SB590885. SB590885 at a low concentration (0.1 μM) increased ERK activity, whereas at a high concentration (1.0 μM), SB590885 suppressed ERK activity (Figures 3F and 3H, Movie S5). This biphasic effect of the Raf inhibitor on ERK activity is consistent with previous studies (Hatzivassiliou et al., 2010; Heidorn et al., 2010; Poulikakos et al., 2010). On the other hand, the frequency of ERK activity pulses was monotonously decreased with the increment of SB590885 concentration (Figure 3I). Importantly, in the presence of SB590885, the width of the ERK activity pulses was significantly extended over 1 hr (Figures 3F and 3J, middle). The prolongation of the ERK activity pulses was reproduced by other Raf inhibitors, PLX-4702 and GDC-0879. Generally, it is known that the activity of the pulse generator determines the pulse shape, which would suggest that Raf is involved in the generation of the pulsatile ERK activation. Meanwhile, an MEK inhibitor, PD184352, decreased the basal ERK activity and the frequency of the ERK activity pulses but did not affect the width of the ERK activity pulses (Figures 3G–3J, Movie S6), which would exclude MEK from the list of potential pulse generators.

We extended the approach with chemical inhibitors to gain further insight into the stochastic ERK activity pulses (Figures 3K and S3C–S3E). An epidermal growth factor receptor (EGFR) inhibitor, PD184352, and a phosphatidylinositol 3-kinase (PI3K) inhibitor, PI-103, markedly reduced the frequency of ERK activity pulses. A protein kinase C (PKC) inhibitor, Go6983, slightly decreased the frequency of ERK activity pulses. However, in contrast to the Raf inhibitor, these three reagents affected the width of ERK activity pulses only minimally. An ATP diphosphatase, Apyrase, increased the pulse width, albeit to an extent much less than did the Raf inhibitor (Figure S3E). Intriguingly, all tested inhibitors of actin cytoskeleton, Latrunculin A, Cytochalasin D, Jasplakinolide, and Brebstatin, induced robust ERK activation (Figure S3F). Thus, actin cytoskeleton also contributes to the generation of the ERK activity pulses.

These observations indicate that the generation of the stochastic ERK activity pulses requires basal activities of EGFR, Ras, PI3K, and Rac1 and intact actin cytoskeleton. Among the signaling molecules examined so far, Raf activity was correlated most prominently with the width of ERK activity pulses, implying that Raf is a key component of the generation of the ERK activity pulses.

## The ERK Activity Pulses Are Propagated to Neighboring Cells

We next focused on the lateral propagation of ERK activity pulses to neighboring cells. At the intermediate cell density

(2.2–4.6 × 10⁴ cells/cm²), ERK activity was reproducibly propagated to adjacent cells (Figure 4A). Cross-correlation analysis of the time course of ERK activity indicated a propagation of ERK activity pulses to neighboring cells with a time delay of 3–6 min (Figure 4B). To gain direct evidence of the propagation of ERK activity pulses to the neighboring cells, we constructed a light-inducible ERK activation system in which *Arabidopsis thaliana* cryptochrome 2 (CRY2)-fused CRaf protein is recruited to the plasma membrane through CRY2 binding to the N-terminal domain of CIB1 (CIBN) in a blue light-dependent manner (Kennedy et al., 2010) (Figure 4C). Here, mCherry-ERK was also expressed to monitor the activation of ERK by nuclear translocation. The resulting mCherry-ERK cells were seeded with the NRK cells expressing the EKAREV FRET biosensor (Figure 4D). The mCherry-ERK2 proteins started to translocate to the nucleus 3–5 min after blue light exposure, followed by the increase in FRET in NRK/EKAREV cells with the time delay of 5–8 min (Figures 4E and 4F, Movie S7), providing the direct evidence of the lateral propagation of ERK activity pulses by the synthetic approach. Importantly, the ERK activation was always transient in NRK/EKAREV cells (Figure 4F, green lines), irrespective of the constitutively high ERK activity in mCherry-ERK2 cells (Figure 4F, red).

To find molecules involved in the lateral propagation of the ERK activity pulses, we screened chemical inhibitors. We found that inhibitors of EGFR and matrix metalloproteinases (MMPs) completely blocked the propagation of the synthetically induced ERK activity pulses (Figures 4G and S4). Inhibitors of PKC and PI3K partially inhibited the ERK activity propagation (Figure S4). This observation strongly argued for the following scenario (Figure 4H): the stochastic ERK activation stimulates a disintegrin and metalloproteases (ADAMs), which cleave membrane-bound ligands of the EGF family. The liberated EGF-family ligands in turn engage EGFR on the neighboring cells and activate ERK in a manner dependent on PKC and PI3K.

Synthetic ERK Activity Pulses Accelerate the Cell Proliferation Rate

Taking advantage of the light-inducible ERK activation system, we further addressed the physiological role of stochastic ERK activation and inactivation. First, we determined the light intensity response of ERK phosphorylation. Under a continuous illumination condition, the half-maximal ERK phosphorylation (LI₅₀) was determined as 12.5 μW/cm² (Figures 5A and 5B). Second, we expressed the Rac1 dominant-negative mutant to suppress the stochastic ERK activity pulses (Figure 3D). Then, to mimic the ERK activity dynamics at the intermediate cell density, the durations of the light and dark periods were set to 20 min and 60 min, respectively, according to the width and frequency of ERK activity pulses at the intermediate cell density (Figure 5C, upper). Continuous light exposure per se did not affect EdU incorporation in the parent NRK-52E cells (Figures 5D and S5). However, intermittent light exposure significantly increased EdU-positive cells (Figure 5D). These results directly demonstrated that the ERK activity pulses accelerated cell proliferation.
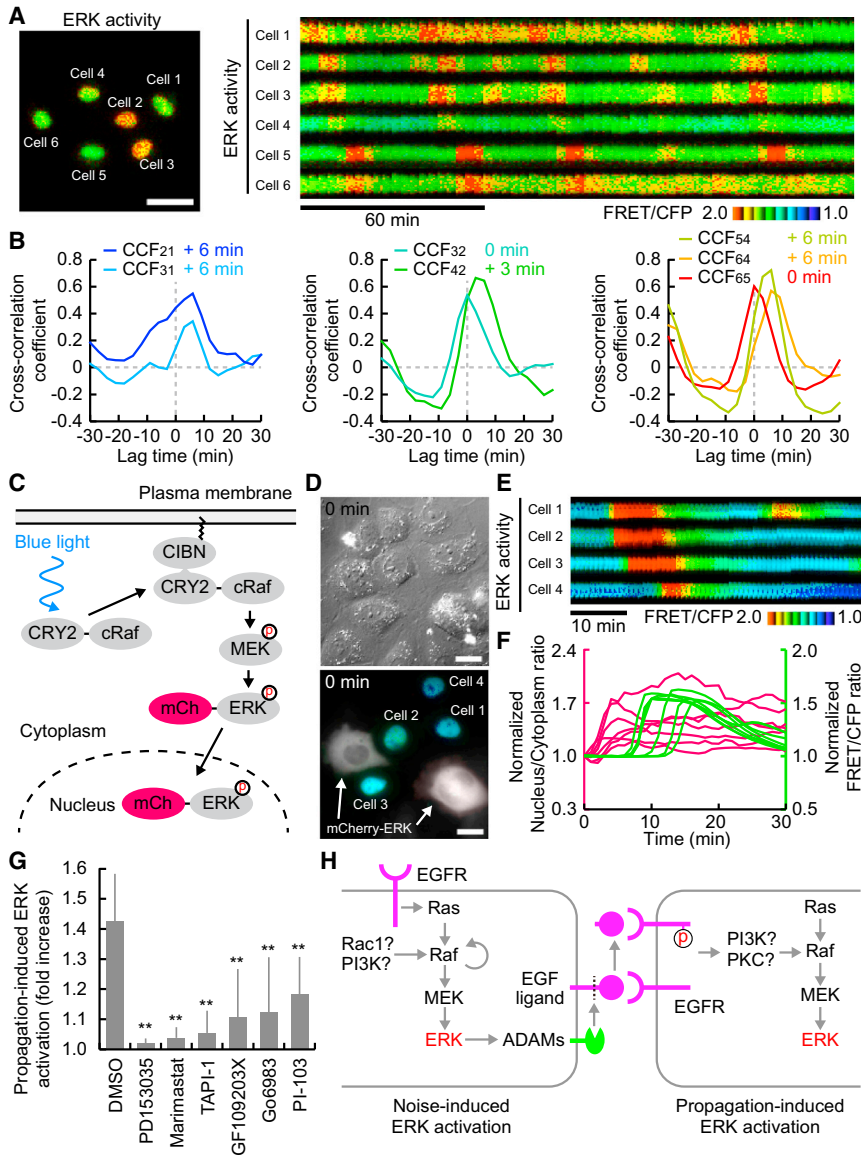
Figure 4. Propagation of ERK Activity

(A) NRK-52E cells expressing EKAREV-NLS were imaged as in Figure 1. Montage images of ERK activity are represented in the indicated cells, demonstrating ERK activity propagation (right).

(B) Cross-correlation analysis of ERK activity in a pair of cells from (A). CCF21 means the cross-correlation function of cell 2 from cell 1. The positive shift of lag time indicates the time delay of ERK activity propagation from cell 2 to cell 1.

(C) Scheme of light-switchable ERK activation system.

(D) NRK-52E cells expressing EKAREV-NLS were cocultured with NRK-52E cells expressing CIBN-EGFP-KRasCT, CRY2-CRaf, FLAG-MEK1, and mCherry-ERK2 (arrows).

(E) ERK activity in the indicated cells from (D) (lower) is shown as montage images.

(F) ERK activities are plotted as a function of time after light-switchable activation. Red and green lines indicate the ratio of mCherry-ERK at the nucleus to that at the cytoplasm and the FRET/CFP ratio, respectively.

(G) Maximal ERK activity (FRET/CFP ratio) after light-induced ERK activity propagation are shown as mean with SD in the presence of the indicated inhibitor: DMSO (n = 35), 1 μM PD153035 (EGFR inhibitor, n = 15), 10 μM Marimastat (MMPs inhibitor, n = 16), 10 μM TAPI-1 (MMPs inhibitor, n = 14), 5 μM GF109203X (PKC inhibitor, n = 16), 5 μM Gö6983 (PKC inhibitor, n = 23), and 10 μM PI-103 (PI3K inhibitor, n = 26). The symbol indicates the results of the t test analysis: **p < 0.01.

(H) A schematic of the propose model of noise-induced ERK activity pulse and its propagation. See also Figure S4.

Mathematical Modeling Reveals a Substantial Role of Cell-to-Cell Propagation and Noise in the Generation of ERK Activity Pulses

As we have shown, the stochastic ERK activity pulses in each cell are generated by either spontaneous firing or propagation from the neighboring cells. Histogram analysis of the inter-pulse interval showed exponential distribution (Figure S6A). Therefore, as is the case with the autonomous excitation of neurons (Kampen, 1981), the ERK activity pulses are generated by stochastic, but not ordered, firing. To quantitatively understand their contribution to the stochastic ERK activity pulses at different cell densities, we derived differential equations in which the parameters were deduced from our experimental data (Figures S6B–S6G; Supplemental Experimental Procedures). We simplified Ras-ERK signaling by taking only two major components, Raf and ERK, into account, making it possible to perform bifurcation analysis in the phase plane. This model includes a

positive feedback reaction by Raf dimerization, a negative feedback suppression of Raf by ERK, noise of Raf, and cell-to-cell propagation of the ERK activity pulses (Figure 6A). In a population of N cells, the level of active Raf ([Raf]) and phospho-ERK ([ERK]) in the i-th cell can be approximated by the following:

$$d[Raf]_i = \left\{ \left(k_{input}(x) + k_{fRaf}[Raf]_i^2 \right) \left(1 - [Raf]_i\right) \right.$$
$$\left. - k_{bRaf}(x)[ERK]_i[Raf]_i \right\} dt + D[Raf]_i \xi_i(t) \quad \text{(Equation 1)}$$
$$+ dt \cdot \kappa \sum_{j=1}^{N} A_{ij} \left([ERK]_j - [ERK]_i \right)_{ERK_j > ERK_i, \ ERK_j > ERK_0}$$

$$d[ERK]_i = \left\{ k_{fERK}[Raf]_i \left(1 - [ERK]_i\right) - k_{bERK}[ERK]_i \right\} dt, \quad \text{(Equation 2)}$$

where $k_{input}(x)$, k_{fRaf}, $k_{bRaf}(x)$, k_{fERK}, and k_{bERK} are rate constants; x is the cell density; D is the noise strength; $\xi_i(t)$ is the white Gaussian noise; κ is the coupling strength; and A_{ij} is the adjacency matrix (for more details, see the Supplemental
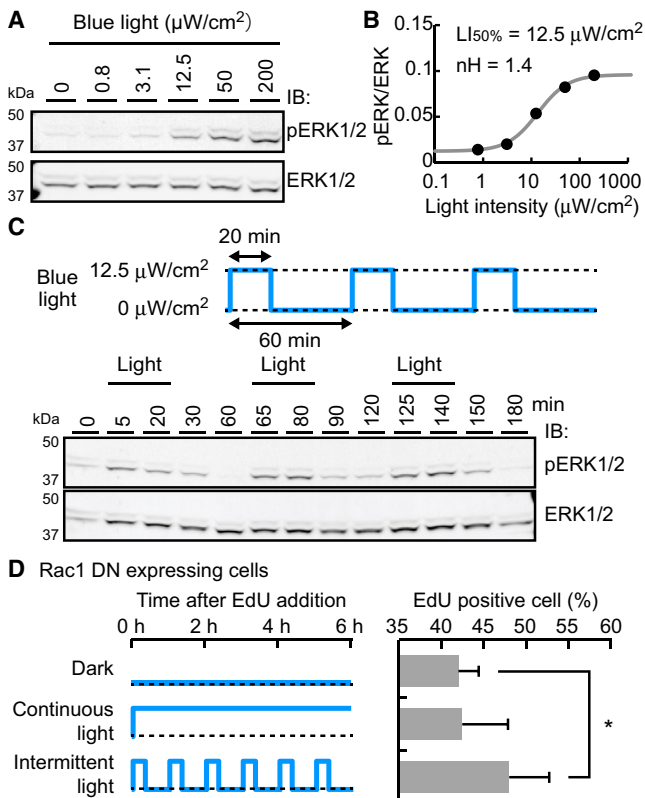
Figure 5. Enhancement of Cell Proliferation by Synthetic ERK Oscillation

(A and B) NRK-52E cells expressing CIBN-EGFP-KRasCT and CRY2-CRaf were exposed to blue light at the indicated light density for 30 min. The cell lysates were subjected to western blotting with anti-pERK (upper) and anti-ERK1/ERK2 (lower) antibodies (A). Ratios of pERK to ERK (black dots) are plotted as a function of light density with a fitted curve (gray line) (B). LI$_{50}$ means the light intensity that induced half maximal ERK activation.

(C) Repetitive blue light exposure (upper) was applied to NRK-52E cells expressing CIBN-EGFP-KRasCT and CRY2-CRaf. The cell lysates were prepared at the indicated time and analyzed by western blotting as in (A).

(D) NRK-52E cells expressing CIBN-EGFP-KRasCT, CRY2-CRaf, and Rac1DN were subject to dark, continuous light and intermittent exposure (light density, 12.5 μW/cm²) for 6 hr in the presence of EdU and analyzed for EdU incorporation (n = 5). The asterisk indicates the results of the t test analysis; *p < 0.05 compared with the dark condition. See also Figure S5.

Experimental Procedures). Intuitively, when noise exceeds a threshold, an ERK activity pulse is fired like neural spikes (Figure 6B). The $k_{input}(x)$ and $k_{bRaf}(x)$ determine the basal and peak ERK activities (Figure 6C). While almost all parameters were derived from the experimental data, there was a single exception in the noise strength, D. Therefore, we estimated the noise strength (Figure 6D) to recapitulate the 20 min width and frequency of the ERK activity pulses at various cell densities (Figures 6E and 6F, Movie S8). This mathematical model could reproduce the relationship between the input stimulation strength and the frequency and amplitude of ERK activity pulses (Albeck et al., 2013); an increase in input stimulation strength increased the frequency, but not the amplitude, of ERK activity pulses (Figures S6H and S6I). In addition, the histogram of inter-

pulse interval in the mathematical model showed exponential distribution (Figure S6J), as observed in experiments (Figure S6A). Intriguingly, the model predicted that only 20% of the total ERK activity pulses were generated by the cell-to-cell propagation of ERK activity pulses, and the remaining 80% were the noise-driven pulses (Figure 6F). This prediction was directly validated by scoring the cell-to-cell propagation-driven ERK activity pulses at various cell densities. The observed fractions of the cell-to-cell propagation-driven ERK activity pulses agreed with the simulation data (Figure 6G); however, at a high cell density we found more cell-to-cell propagation-driven ERK activity pulses than predicted. This could have been due to another mechanism of ERK activity propagation from the neighboring cells; we observed that dead cells seemed to secret soluble factor(s) that activated ERK in neighboring cells (Figure S1G) and that such cell death was frequently observed at the high cell density.

RNA-Seq Analysis Identifies Genes Regulated Specifically by the ERK Activity Pulses

Finally, we attempted to identify genes that were up- or downregulated by the ERK activity pulses. To this end, the light-switchable ERK activation system was utilized again (Figures 4C and 5D). We isolated mRNA from cells cultured under a dark (basal ERK activity), continuous light (sustained ERK activation), or intermittent light (ERK activity pulse) condition. RNA-seq analysis identified genes expressed differentially in cells with the sustained ERK activation or cells with the ERK activity pulses in comparison to cells with the basal ERK activity (Figures 7A and 7B). While the sustained ERK activity upregulated the mRNA expression of approximately 100 genes, the ERK activity pulses upregulated the mRNA expression of only 10 genes, among which *Fos*, *Egr1*, *Dusp1*, *Ier2*, and *Fgf21* were specific to the ERK activity pulses (Figure 7C). Only one gene, *Fam111a*, was downregulated by the ERK activity pulses, whereas 66 genes were downregulated by the sustained ERK activation (Figure 7D).

We analyzed the promoter regions for these differentially expressed genes by using Gene Set Enrichment Analysis software for the sake of identifying the transcription factors responsible for the ERK activity pulse-dependent transcriptional changes. Intriguingly, we found that the binding sites of serum responsive factor (SRF) were enriched in the promoter regions of the ERK activity pulse-induced genes (Figure 7E). On the other hand, activator protein 1 (AP1)-binding sites and transcription enhancer factor (TEF1)-binding sites were enriched in sustained ERK-dependent upregulated and downregulated genes (Figures 7F and 7G). These results provided a mechanistic insight into how the stochastic ERK dynamics were decoded through transcriptional regulation.

DISCUSSION

Here, we have demonstrated that the cell density-dependent control of proliferation in mammalian cells is associated with the frequency of the ERK activity pulses, which consist of pulses from both spontaneous firing and cell-to-cell propagation. Single-cell analyses with fluorescent proteins have revealed the
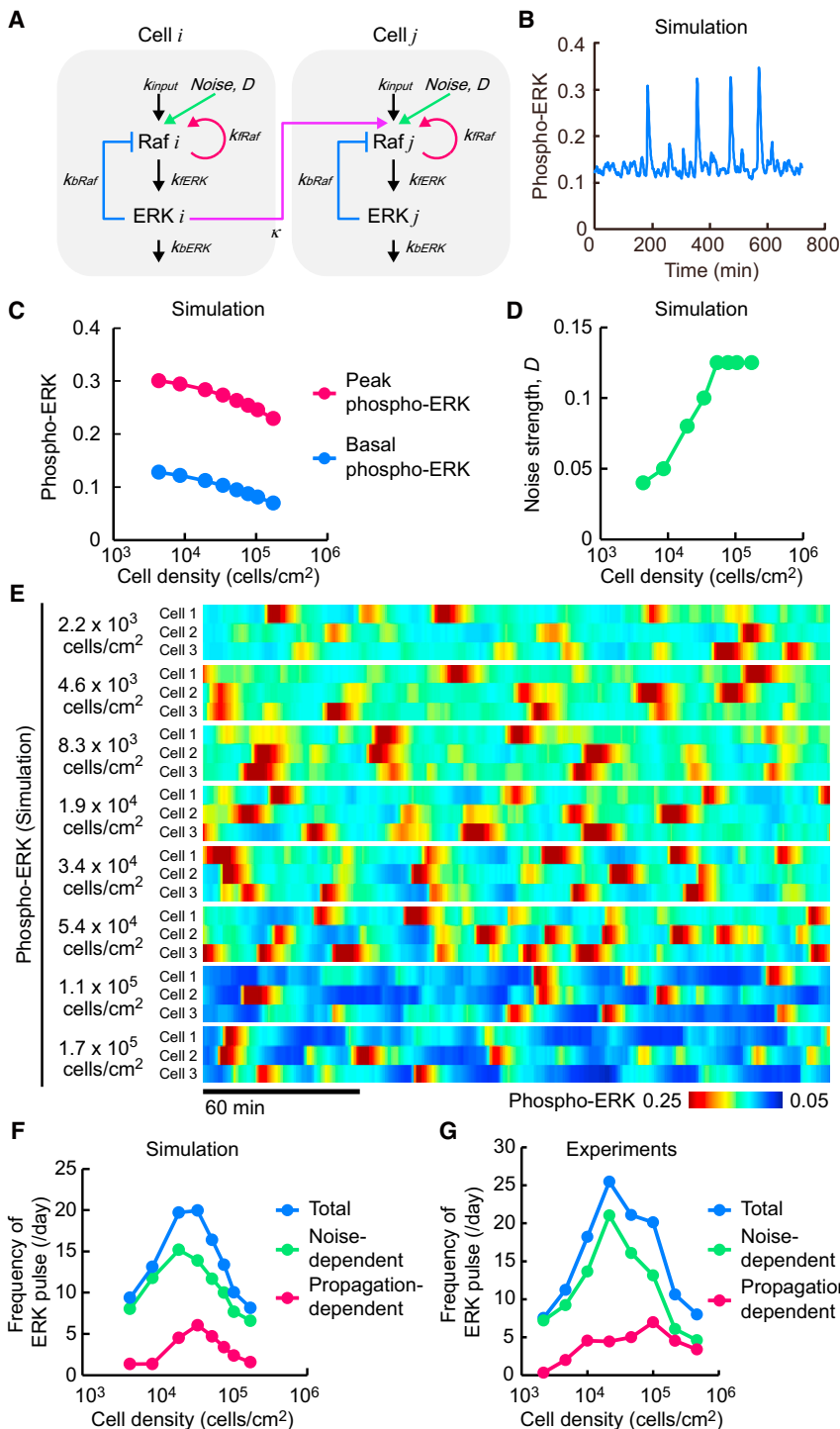
Figure 6. Mathematical Modeling of Multi-cellular Stochastic ERK Dynamics

(A) Schematic representation of the Raf-ERK two-component model, including positive (k_{fRaf}) and negative (k_{bRaf}) feedbacks with noise (D) and propagation (κ).

(B) Representative excitatory dynamics of phospho-ERK.

(C) The fractions of basal (blue) and peak (red) levels of phospho-ERK are plotted as a function of cell density.

(D) Noise strength was estimated in order to reproduce the relationship between cell density and frequency of ERK pulses as in Figure 2C.

(E) Fractions of phospho-ERK in three representative cells at each cell density are plotted as montage images.

(F) Prediction of the fraction of ERK pulse frequency driven by noise (green) and propagation (red) in total ERK pulse frequency (blue) based on numerical simulation.
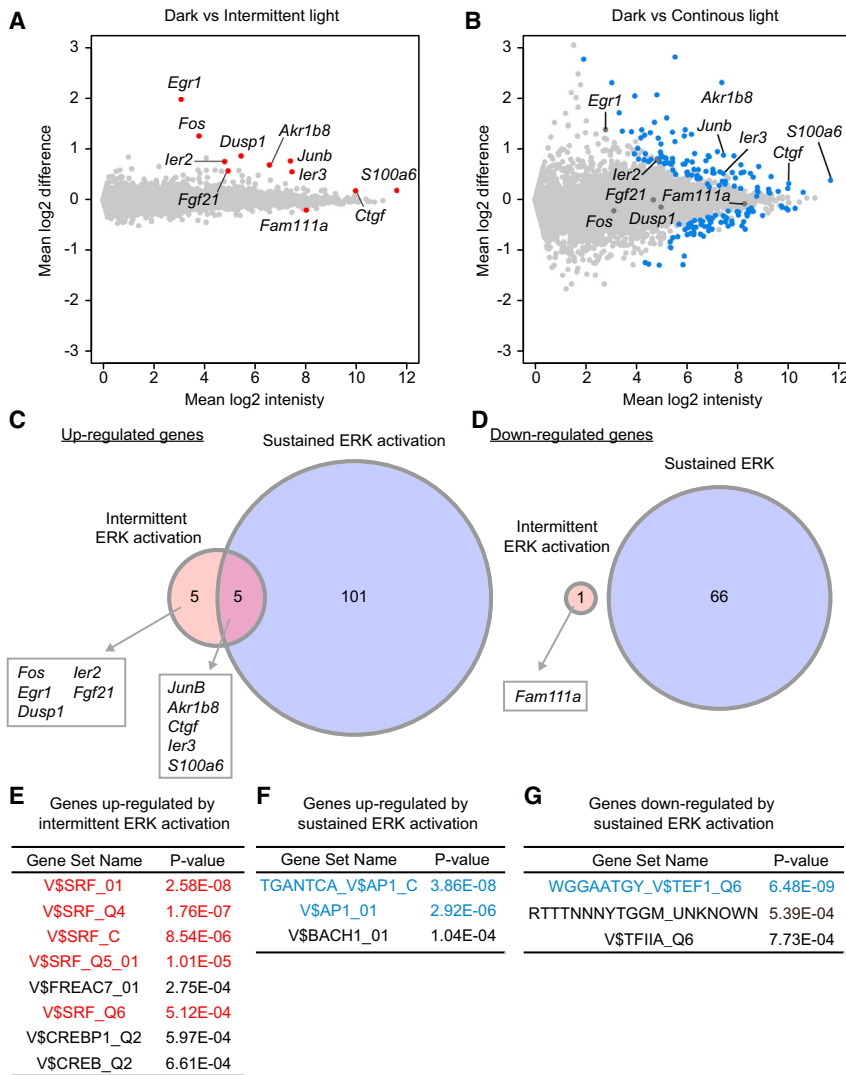
(G) Validation of fractions of ERK pulses driven by noise (green) and propagation (red) by image processing from time-lapse FRET imaging. See also Figure S6 and Supplemental Experimental Procedures.

stochastic ERK activity pulses as found in our study. There are two possible explanations for this discrepancy. First, the preceding studies observed ERK activation after various triggers, whereas we observed cells growing in culture medium containing 10% FBS. Our condition may be similar to the medium containing a low concentration of growth factor, with which Albeck et al. (2013) showed repetitive ERK activation pulses after stimulation. Second, the ERK activation was monitored by nuclear translocation of ERK-GFP. For the manifestation of nuclear translocation of ERK, a substantial amount of ERK must be phosphorylated, and this can be achieved only by stimulation with growth factors or ER stress. On the other hand, the EKAREV-NLS developed in our laboratory could monitor an increase in phospho-ERK as small as 5% (Figure S1), enabling us to visualize the stochastic ERK activation in a stable state.

What causes the spontaneous firing of the ERK activity pulses? The stochastic excitable dynamical system requires noise and feedback reaction(s) (Lindner et al., 2004). We assume that Raf is the target of noise to induce stochastic ERK dynamics for the following reasons. First, we did not find any pulses of Ras activity in the normal growth condition. Nevertheless, a dominant-negative mutant of Ras suppressed the ERK activity

oscillatory dynamics of signaling molecules such as p53, ERK, and NF-κB (Lahav et al., 2004; Shankaran et al., 2009; Tay et al., 2010). In the case of ERK, several research groups have observed ERK oscillation in response to growth factors (Nakayama et al., 2008; Shankaran et al., 2009) or endoplasmic reticulum (ER) stress (Zhang et al., 2011). All of the previous studies reported ordered oscillatory ERK activation, but not

Figure 7. Gene Expression Regulation upon Intermittent or Continuous ERK Activation

(A and B) MA plot (the difference of average log intensities and the average of log intensities) of intermittent (A) or continuous (B) light exposure in comparison to dark condition in NRK-52E cells expressing CIBN-EGFP-KRasCT and CRY2-CRaf (n = 2). Red and blue dots represent differentially expressed genes.

(C and D) Venn diagrams represent upregulated genes (C) and downregulated genes (D) upon intermittent (red) and continuous (blue) light exposures in comparison to those under a dark condition.

(E–G) Promoter analysis for the upregulated gene by intermittent light exposure (E), the upregulated gene by continuous light exposure (F), and the downregulated gene by continuous light exposure (G).

E Genes up-regulated by intermittent ERK activation

Gene Set Name	P-value
V$SRF_01	2.58E-08
V$SRF_Q4	1.76E-07
V$SRF_C	8.54E-06
V$SRF_Q5_01	1.01E-05
V$FREAC7_01	2.75E-04
V$SRF_Q6	5.12E-04
V$CREBP1_Q2	5.97E-04
V$CREB_Q2	6.61E-04

F Genes up-regulated by sustained ERK activation

Gene Set Name	P-value
TGANTCA_V$AP1_C	3.86E-08
V$AP1_01	2.92E-06
V$BACH1_01	1.04E-04

G Genes down-regulated by sustained ERK activation

Gene Set Name	P-value
WGGAATGY_V$TEF1_Q6	6.48E-09
RTTTNNNYTGGM_UNKNOWN	5.39E-04
V$TFIIA_Q6	7.73E-04

activities of EGFR and Ras are prerequisites for this phenomenon (Figures 3D and 3K). Thus, we suggest that the stochasticity of the signals converging on Raf may be responsible for the generation of ERK activity pulses. Furthermore, our mathematical model shows a correlation between the noise strength and the cell density (Figure 6D), which may imply the link from physical tension to the Raf activity. Therefore, the spontaneous firing of the ERK activity pulses seems to be evoked by the internal and/or external noises in the upstream signaling molecules.

One of the findings in this study is the lateral propagation of ERK activity pulses (Figure 4). Inhibitors of EGFR or MMPs completely abolished the lateral propagation of ERK activity pulses (Figures 4G and S4A). It has been reported that ERK phosphorylates and activates ADAM17, which in turn induces ectodomain cleavage of membrane proteins including EGF-family proteins (Díaz-Rodríguez et al., 2002; Umata et al., 2001). Our observation strongly argues for the following scenario: the stochastic activation of ERK drives ADAMs activation, thereby liberating the EGF-family proteins to engage EGFR of the neighboring cells. Then, why did we fail to observe stochastic Ras activation (Figures 3B and 3C), which should be naturally evoked after EGFR activation? The involvement of PKC and PI3K in the ERK activity propagation (Figure 4G) may reconcile the apparent contradiction. PKC and PI3K-activated PAK are known to phosphorylate and activate Raf in the absence of Ras activation. Alternatively, Ras activation induced by the local EGFR activation, which would occur only at the cell-to-cell contact region, may be below the sensitivity level of the RaichuEV-Ras.

There have been several reports on the feedback regulations in the Ras-ERK pathway, which may account for the generation of the ERK activity pulses. In considering these regulations, we first excluded the possibility of a transcription-dependent

pulses, strongly suggesting that the noise is evoked at the level of Raf binding to Ras. Second, the Raf concentration, which was 13 nM for CRaf in the cytoplasm, is much lower than the concentrations of Ras, MEK, and ERK, which were on the order of 1.0 μm in HeLa cells (Fujioka et al., 2006). The low concentration of CRaf could have conferred a susceptibility to noise. Third, cell lines known to harbor active Raf mutations did not show the ERK activity pulses (Figure S1D). Fourth, Raf is regulated primarily by Ras, but it is also modulated by multiple factors, including kinases (Kolch, 2000), scaffold proteins (Kolch, 2005), and calcium ions (Terai and Matsuda, 2006), which alter the conformation of Raf. It is possible that the fluctuation of activities or concentrations of these modulatory factors act as the source of noise. In support of this note, stochastic ERK activity pulses were suppressed by the inhibition of PI3K or Rac1, both of which are known to regulate Raf by means of p21-activating kinase (PAK). Needless to say, the stochastic nature of the input signals, i.e., serum or other growth factors, will also contribute to the firing of the stochastic ERK activation pulses because the basal

feedback mechanism because of the short pulse width of 20–30 min. Second, the negative feedback regulation from ERK to Sos1 (Cherniack et al., 1995) was also neglected because Ras did not show stochastic activation. Thus, we employed the negative feedback phosphorylation of CRaf by ERK in the model (Figure 6) (Dougherty et al., 2005). We also implemented a positive feedback through Raf dimerization. The importance of Raf dimerization for Raf activation has been demonstrated, for example, by the fact that low concentrations of Raf inhibitors induced Raf dimerization and resulted in paradoxical ERK activation (Hatzivassiliou et al., 2010; Heidorn et al., 2010; Poulikakos et al., 2010). In agreement with this finding, we found that a low concentration of a Raf inhibitor prolonged the width of the ERK activity pulses (Figure 3). As a result of Raf dimerization, the positive feedback confers excitability to the model. Previously, it has been shown that oscillations of MAPK cascades could be generated by negative feedback and ultrasensitivity of ERK phosphorylation by MEK in *Xenopus* oocytes (Kholodenko, 2000). However, we did not employ this model because ERK is processively phosphorylated by MEK in mammalian cells (Aoki et al., 2011). Future studies will be needed to evaluate the role of the possible feedback regulations in the stochastic generation of ERK activation pulse.

By RNA-seq analysis, we found that ERK activity pulses, but not the sustained ERK activation, induce SRF-regulated genes such as *Fos* and *Egr1*. Interestingly, Zwang et al. (2011) have reported that two pulses of EGF stimulation induced *Egr1* gene expression in mammary epithelial cells, leading to a commitment to cell proliferation. Phosphorylation of Elk-1 by ERK or RSK, an ERK-regulated kinase, induces Elk-1 binding to SRF, and thereby results in an increase in SRF transcriptional activity (Buchwalter et al., 2004). In addition, nuclear accumulation of phosphorylated ERK has been shown to be required for Elk-1 phosphorylation (Torii et al., 2004). Importantly, several studies have reported that sustained ERK activation induced by TPA or oncogenic mutants of Ras or BRaf induces expression of dual-specificity phosphatase in the nucleus and suppresses nuclear ERK activity (Cagnol and Rivard, 2013; Caunt et al., 2008). Thus, ERK activity pulses, but not the sustained ERK activation, maintain the phosphorylation of ERK substrates in the nucleus, leading to constitutive activation of SRF and thereby promoting cell growth.

Recently, by using EKAREV-NLS, Albeck and Brugge have shown that the frequency of the ERK activity pulses depend on the concentration of EGF in mammary epithelial cells and proposed that the integration of ERK activity over a period of 2–3 days causes the accumulation of downstream transcription factors and thereby progression of the cell cycle (Albeck et al., 2013). In their mathematical model, the ERK activation is required for the accumulation of the transcription factors. If so, sustained ERK activation would promote cell proliferation more efficiently than do ERK activity pulses. However, this is not the case, at least in NRK-52E cells, as shown in Figure 4. This inconsistency would suggest the involvement of other signaling pathways in the promotion of cell proliferation. The light-induced ERK activation system adopted in this study specifically activates ERK by CRaf activation, and this might be the reason why the intermittent ERK activation resulted in only a 5% increment in cell proliferation rate (Figure 5D). On the other hand, the EGF treatment adopted by Albeck and Brugge stimulates not only ERK, but also other signaling molecules, such as PI3K and Akt. In agreement with this idea, it has been shown that EGF-induced Akt activation plays a positive role in cell proliferation through downregulation of p53 (Zwang et al., 2011). Thus, in the presence of Akt activation, sustained ERK activation may also promote cell growth.

We would like to argue that the stochastic ERK activity pulses control, to some degree, the cell density-dependent cell proliferation. A future work should address how cells decode the information of cell density encoded as a frequency of ERK pulses and how the temporal ERK dynamics are processed by downstream molecules of ERK. An understanding of the quantitative relationship between ERK signaling and cell proliferation would provide a useful framework to predict the clinical efficacy of drugs targeting the Ras-ERK pathway to impede the proliferation of cancer cells.

EXPERIMENTAL PROCEDURES

Establishment of Stable Cell Lines

To generate cell lines stably expressing FRET biosensors, we utilized a PiggyBac transposon system (Aoki et al., 2012). For establishment of stable cell lines expressing ectopic proteins (except FRET biosensors), we employed a retroviral system for other proteins. The ectopic protein was introduced into NRK-52E cells by retroviruses produced from BOSC23 cells, which had been transfected with hyg-EcoVR, the packaging plasmid pGP (Akagi et al., 2003), and the envelope plasmid pCMV-VSVG-RSV-Rev. Finally, we obtained NRK-52E cells expressing CIBN-EGFP-KRasCT and CRY2-CRaf.

Cell Proliferation Assay

Cells were seeded onto glass substrates. At 12 hr after seeding, cells were cultured in the presence of 10% FBS and 5-ethynyl-20-deoxyuridine (EdU) for 12 hr (Figure 2) or 6 hr (Figure 5) and then fixed and assayed for EdU incorporation using an EdU assay kit (Invitrogen) according to the manufacturer's instructions. For EdU imaging, more than 16 fields per well were captured at 20× magnification. The percentage of EdU-positive cells in total cells, which were identified by Hoechst 33342 nuclei staining, was analyzed by MetaMorph software (Universal Imaging).

Time-Lapse FRET Imaging

FRET images were obtained and processed using essentially the same conditions and procedures as previously reported (Aoki and Matsuda, 2009). Confocal and two-photon excitation microscopy for time-lapse imaging of cysts and mammary gland was performed as previously described (Kamioka et al., 2012; Sakurai et al., 2012). All animal care measures and experiments complied with Japanese community standards on the care and use of laboratory animals, which were approved by Kyoto University.

Light-Switchable ERK Activation System

NRK-52E cells expressing CIBN-EGFP-KRasCT and CRY2-CRaf were seeded onto 35 mm glass-based dishes. At 1 day after seeding, the cells were serum starved for 3 days with Medium 199 supplemented with 0.1% BSA. At 3 days after serum starvation, the cells were maintained under conditions of dark, continuous, and intermittent blue light exposure in a CO_2 incubator (SANYO Electric Co.). LED-41VIS470F (Optocode Co.) was used as a blue light source. The density of light was measured by an optical power meter TQ8210 (Advantest).

Numerical Simulation

Cross correlation analysis (Figure 3B) and numerical simulation (Figure 5) were implemented by MATLAB software (MathWorks). The stochastic differential equations were numerically solved by the Euler-Maruyama method (Kloeden

and Platen, 1992). The details are described in the Supplemental Experimental Procedures.

Library Preparation and Sequencing

An Illumina TruSeq DNA Sample Preparation Kit was used to generate (50 bp paired-end cDNA) sequencing libraries by following the manufacturer's protocol. The libraries were loaded onto flow cell channels for sequencing on an Illumina HiSeq 2000 at the Omics Science Center (OSC) RIKEN Yokohama Institute.

Mapping and Computation of Expression Values

Sequence reads of each data set were aligned to the rat genome (rn4, Nov. 2004, version 3.4) using the Burrows-Wheeler Aligner's Smith-Waterman Alignment program (v.0.5.9; Li and Durbin, 2009). The DEGseq package in R software (Li and Durbin, 2009) computed the gene expression for the transcripts in the samples using the UCSC rn4 transcriptome (ftp://hgdownload.cse.ucsc.edu/goldenPath/hg19/database/) as a reference. The reads per kilobase (kb) of exon model per million mapped reads (RPKM) method (Mortazavi et al., 2008) was used for normalization with the total mapped reads count and the gene length to quantitate the level of gene expression. Differentially expressed genes were identified by the DEGseq package, using a p value < 0.05 as the threshold. Fisher's exact test was chosen to measure the significance of the gene expression differences.

ACCESSION NUMBERS

RNA-seq data described herein are deposited in the Sequence Read Archive (SRA) database under accession numbers DRX0012476, DRX0012477, DRX0012478, DRX0012479, DRX0012480, and DRX0012481.

SUPPLEMENTAL INFORMATION

Supplemental Information includes Supplemental Experimental Procedures, six figures, and eight movies and can be found with this article online at http://dx.doi.org/10.1016/j.molcel.2013.09.015.

REFERENCES

Abercrombie, M. (1979). Contact inhibition and malignancy. Nature *281*, 259–262.

Akagi, T., Sasai, K., and Hanafusa, H. (2003). Refractory nature of normal human diploid fibroblasts with respect to oncogene-mediated transformation. Proc. Natl. Acad. Sci. USA *100*, 13567–13572.

Albeck, J.G., Mills, G.B., and Brugge, J.S. (2013). Frequency-modulated pulses of ERK activity transmit quantitative proliferation signals. Mol. Cell *49*, 249–261.

Aoki, K., and Matsuda, M. (2009). Visualization of small GTPase activity with fluorescence resonance energy transfer-based biosensors. Nat. Protoc. *4*, 1623–1631.

Aoki, K., Yamada, M., Kunida, K., Yasuda, S., and Matsuda, M. (2011). Processive phosphorylation of ERK MAP kinase in mammalian cells. Proc. Natl. Acad. Sci. USA *108*, 12675–12680.

Aoki, K., Komatsu, N., Hirata, E., Kamioka, Y., and Matsuda, M. (2012). Stable expression of FRET biosensors: a new light in cancer research. Cancer Sci. *103*, 614–619.

Buchwalter, G., Gross, C., and Wasylyk, B. (2004). Ets ternary complex transcription factors. Gene *324*, 1–14.

Cagnol, S., and Rivard, N. (2013). Oncogenic KRAS and BRAF activation of the MEK/ERK signaling pathway promotes expression of dual-specificity phosphatase 4 (DUSP4/MKP2) resulting in nuclear ERK1/2 inhibition. Oncogene *32*, 564–576.

Cai, L., Dalal, C.K., and Elowitz, M.B. (2008). Frequency-modulated nuclear localization bursts coordinate gene regulation. Nature *455*, 485–490.

Caunt, C.J., Armstrong, S.P., Rivers, C.A., Norman, M.R., and McArdle, C.A. (2008). Spatiotemporal regulation of ERK2 by dual specificity phosphatases. J. Biol. Chem. *283*, 26612–26623.

Cherniack, A.D., Klarlund, J.K., Conway, B.R., and Czech, M.P. (1995). Disassembly of Son-of-sevenless proteins from Grb2 during p21ras desensitization by insulin. J. Biol. Chem. *270*, 1485–1488.

Díaz-Rodríguez, E., Montero, J.C., Esparís-Ogando, A., Yuste, L., and Pandiella, A. (2002). Extracellular signal-regulated kinase phosphorylates tumor necrosis factor alpha-converting enzyme at threonine 735: a potential role in regulated shedding. Mol. Biol. Cell *13*, 2031–2044.

Dougherty, M.K., Müller, J., Ritt, D.A., Zhou, M., Zhou, X.Z., Copeland, T.D., Conrads, T.P., Veenstra, T.D., Lu, K.P., and Morrison, D.K. (2005). Regulation of Raf-1 by direct feedback phosphorylation. Mol. Cell *17*, 215–224.

Eagle, H., and Levine, E.M. (1967). Growth regulatory effects of cellular interaction. Nature *213*, 1102–1106.

Fujioka, A., Terai, K., Itoh, R.E., Aoki, K., Nakamura, T., Kuroda, S., Nishida, E., and Matsuda, M. (2006). Dynamics of the Ras/ERK MAPK cascade as monitored by fluorescent probes. J. Biol. Chem. *281*, 8917–8926.

Hao, N., and O'Shea, E.K. (2012). Signal-dependent dynamics of transcription factor translocation controls gene expression. Nat. Struct. Mol. Biol. *19*, 31–39.

Hatzivassiliou, G., Song, K., Yen, I., Brandhuber, B.J., Anderson, D.J., Alvarado, R., Ludlam, M.J., Stokoe, D., Gloor, S.L., Vigers, G., et al. (2010). RAF inhibitors prime wild-type RAF to activate the MAPK pathway and enhance growth. Nature *464*, 431–435.

Heidorn, S.J., Milagre, C., Whittaker, S., Nourry, A., Niculescu-Duvas, I., Dhomen, N., Hussain, J., Reis-Filho, J.S., Springer, C.J., Pritchard, C., and Marais, R. (2010). Kinase-dead BRAF and oncogenic RAS cooperate to drive tumor progression through CRAF. Cell *140*, 209–221.

Kahan, C., Seuwen, K., Meloche, S., and Pouysségur, J. (1992). Coordinate, biphasic activation of p44 mitogen-activated protein kinase and S6 kinase by growth factors in hamster fibroblasts. Evidence for thrombin-induced signals different from phosphoinositide turnover and adenylylcyclase inhibition. J. Biol. Chem. *267*, 13369–13375.

Kamioka, Y., Sumiyama, K., Mizuno, R., Sakai, Y., Hirata, E., Kiyokawa, E., and Matsuda, M. (2012). Live imaging of protein kinase activities in transgenic mice expressing FRET biosensors. Cell Struct. Funct. *37*, 65–73.

Kampen, N.G.v. (1981). Stochastic processes in physics and chemistry. (Amsterdam: Elsevier).

Kennedy, M.J., Hughes, R.M., Peteya, L.A., Schwartz, J.W., Ehlers, M.D., and Tucker, C.L. (2010). Rapid blue-light-mediated induction of protein interactions in living cells. Nat. Methods *7*, 973–975.

Kholodenko, B.N. (2000). Negative feedback and ultrasensitivity can bring about oscillations in the mitogen-activated protein kinase cascades. Eur. J. Biochem. 267, 1583–1588.

Kloeden, P.E., and Platen, E. (1992). Numerical Solution of Stochastic Differential Equations, Volume 23. (Berlin, Germany: Springer).

Kolch, W. (2000). Meaningful relationships: the regulation of the Ras/Raf/MEK/ERK pathway by protein interactions. Biochem. J. 351, 289–305.

Kolch, W. (2005). Coordinating ERK/MAPK signalling through scaffolds and inhibitors. Nat. Rev. Mol. Cell Biol. 6, 827–837.

Komatsu, N., Aoki, K., Yamada, M., Yukinaga, H., Fujita, Y., Kamioka, Y., and Matsuda, M. (2011). Development of an optimized backbone of FRET biosensors for kinases and GTPases. Mol. Biol. Cell 22, 4647–4656.

Lahav, G., Rosenfeld, N., Sigal, A., Geva-Zatorsky, N., Levine, A.J., Elowitz, M.B., and Alon, U. (2004). Dynamics of the p53-Mdm2 feedback loop in individual cells. Nat. Genet. 36, 147–150.

Li, H., and Durbin, R. (2009). Fast and accurate short read alignment with Burrows-Wheeler transform. Bioinformatics 25, 1754–1760.

Li, S., Gerrard, E.R., Jr., and Balkovetz, D.F. (2004). Evidence for ERK1/2 phosphorylation controlling contact inhibition of proliferation in Madin-Darby canine kidney epithelial cells. Am. J. Physiol. Cell Physiol. 287, C432–C439.

Lindner, B., García-Ojalvo, J., Neiman, A., and Schimansky-Geier, L. (2004). Effects of noise in excitable systems. Physics Reports 392, 321–424.

Liu, W.F., Nelson, C.M., Pirone, D.M., and Chen, C.S. (2006). E-cadherin engagement stimulates proliferation via Rac1. J. Cell Biol. 173, 431–441.

Marshall, C.J. (1995). Specificity of receptor tyrosine kinase signaling: transient versus sustained extracellular signal-regulated kinase activation. Cell 80, 179–185.

Mortazavi, A., Williams, B.A., McCue, K., Schaeffer, L., and Wold, B. (2008). Mapping and quantifying mammalian transcriptomes by RNA-Seq. Nat. Methods 5, 621–628.

Murphy, L.O., Smith, S., Chen, R.H., Fingar, D.C., and Blenis, J. (2002). Molecular interpretation of ERK signal duration by immediate early gene products. Nat. Cell Biol. 4, 556–564.

Nakayama, K., Satoh, T., Igari, A., Kageyama, R., and Nishida, E. (2008). FGF induces oscillations of Hes1 expression and Ras/ERK activation. Curr. Biol. 18, R332–R334.

Navarro, P., Gómez, M., Pizarro, A., Gamallo, C., Quintanilla, M., and Cano, A. (1991). A role for the E-cadherin cell-cell adhesion molecule during tumor progression of mouse epidermal carcinogenesis. J. Cell Biol. 115, 517–533.

Nishida, E., and Gotoh, Y. (1993). The MAP kinase cascade is essential for diverse signal transduction pathways. Trends Biochem. Sci. 18, 128–131.

Pagès, G., Lenormand, P., L'Allemain, G., Chambard, J.C., Meloche, S., and Pouysségur, J. (1993). Mitogen-activated protein kinases p42mapk and p44mapk are required for fibroblast proliferation. Proc. Natl. Acad. Sci. USA 90, 8319–8323.

Poulikakos, P.I., Zhang, C., Bollag, G., Shokat, K.M., and Rosen, N. (2010). RAF inhibitors transactivate RAF dimers and ERK signalling in cells with wild-type BRAF. Nature 464, 427–430.

Qi, M., and Elion, E.A. (2005). MAP kinase pathways. J. Cell Sci. 118, 3569–3572.

Roskoski, R., Jr. (2012). ERK1/2 MAP kinases: structure, function, and regulation. Pharmacol. Res. 66, 105–143.

Sakurai, A., Matsuda, M., and Kiyokawa, E. (2012). Activated Ras protein accelerates cell cycle progression to perturb Madin-Darby canine kidney cystogenesis. J. Biol. Chem. 287, 31703–31711.

Sasagawa, S., Ozaki, Y., Fujita, K., and Kuroda, S. (2005). Prediction and validation of the distinct dynamics of transient and sustained ERK activation. Nat. Cell Biol. 7, 365–373.

Shankaran, H., Ippolito, D.L., Chrisler, W.B., Resat, H., Bollinger, N., Opresko, L.K., and Wiley, H.S. (2009). Rapid and sustained nuclear-cytoplasmic ERK oscillations induced by epidermal growth factor. Mol. Syst. Biol. 5, 332.

St Croix, B., Sheehan, C., Rak, J.W., Flørenes, V.A., Slingerland, J.M., and Kerbel, R.S. (1998). E-Cadherin-dependent growth suppression is mediated by the cyclin-dependent kinase inhibitor p27(KIP1). J. Cell Biol. 142, 557–571.

Tay, S., Hughey, J.J., Lee, T.K., Lipniacki, T., Quake, S.R., and Covert, M.W. (2010). Single-cell NF-kappaB dynamics reveal digital activation and analogue information processing. Nature 466, 267–271.

Terai, K., and Matsuda, M. (2006). The amino-terminal B-Raf-specific region mediates calcium-dependent homo- and hetero-dimerization of Raf. EMBO J. 25, 3556–3564.

Torii, S., Kusakabe, M., Yamamoto, T., Maekawa, M., and Nishida, E. (2004). Sef is a spatial regulator for Ras/MAP kinase signaling. Dev. Cell 7, 33–44.

Umata, T., Hirata, M., Takahashi, T., Ryu, F., Shida, S., Takahashi, Y., Tsuneoka, M., Miura, Y., Masuda, M., Horiguchi, Y., and Mekada, E. (2001). A dual signaling cascade that regulates the ectodomain shedding of heparin-binding epidermal growth factor-like growth factor. J. Biol. Chem. 276, 30475–30482.

Viñals, F., and Pouysségur, J. (1999). Confluence of vascular endothelial cells induces cell cycle exit by inhibiting p42/p44 mitogen-activated protein kinase activity. Mol. Cell. Biol. 19, 2763–2772.

Wayne, J., Sielski, J., Rizvi, A., Georges, K., and Hutter, D. (2006). ERK regulation upon contact inhibition in fibroblasts. Mol. Cell. Biochem. 286, 181–189.

Zhang, H., Zhao, Y., Tian, T., Paton, A.W., Paton, J.C., and Kitamura, M. (2011). Oscillation of mitogen-activated protein kinases in response to endoplasmic reticulum stress. Anal. Biochem. 417, 292–294.

Zwang, Y., Sas-Chen, A., Drier, Y., Shay, T., Avraham, R., Lauriola, M., Shema, E., Lidor-Nili, E., Jacob-Hirsch, J., Amariglio, N., et al. (2011). Two phases of mitogenic signaling unveil roles for p53 and EGR1 in elimination of inconsistent growth signals. Mol. Cell 42, 524–535.